Science of the Total Environment 899 (2023) 165454

Contents lists available at ScienceDirect

Science of the Total Environment

journal homepage: www.elsevier.com/locate/scitotenv

Effect of ventilation strategy on performance of upper-room ultraviolet germicidal irradiation (UVGI) system in a learning environment

Seongjun Park [a], Richard Mistrick [b], William Sitzabee [c], Donghyun Rim [d,*]

[a] Department of Architectural Engineering, Pennsylvania State University, United States of America
[b] Architectural Engineering Department, Pennsylvania State University, 104 Engineering Unit A, University Park, PA 16802, United States of America
[c] Pennsylvania State University, 201 Physical Plant Building, University Park, PA 16802, United States of America
[d] Architectural Engineering Department, Pennsylvania State University, 222 Engineering Unit A, University Park, PA 16802, United States of America

ARTICLE INFO

Editor: Philip K. Hopke

Keywords:
Indoor air quality
Airborne infection
COVID-19 control
Ventilation effectiveness
Indoor airflow
Computational fluid dynamics (CFD)

ABSTRACT

Upper-room ultraviolet germicidal irradiation (UVGI) system is recently in the limelight as a potentially effective method to mitigate the risk of airborne virus infection in indoor environments. However, few studies quantitatively evaluated the relationship between ventilation effectiveness and virus disinfection performance of a UVGI system. The objective of this study is to investigate the effects of ventilation strategy on detailed airflow distributions and UVGI disinfection performance in an occupied classroom. Three-dimensional computational fluid dynamics (CFD) simulations were performed for representative cooling, heating, and ventilation scenarios. The results show that when the ventilation rate is 1.1 h^{-1} (the minimum ventilation rate based on ASHRAE 62.1), enhancing indoor air circulation with the mixing fan notably improves the UVGI disinfection performance, especially for cooling with displacement ventilation and all-air-heating conditions. However, increasing indoor air mixing yields negligible effect on the disinfection performance for forced-convection cooling condition. The results also reveal that regardless of indoor thermal condition, disinfection effectiveness of a UVGI system increases as ventilation effectiveness is close to unity. Moreover, when the room average air speed is >0.1 m/s, upper-room UVGI system could yield about 90% disinfection effect for the aerosol size of 1 μm–10 μm. The findings of this study imply that upper-room UVGI systems in indoor environments (i.e., classrooms, hospitals) should be designed considering ventilation strategy and occupancy conditions, especially for occupied buildings with insufficient air mixing throughout the space.

1. Introduction

As scientific evidence supports airborne transmission of COVID-19, the role of ventilation in buildings has been highlighted (Morawska and Milton, 2020; Morawska and Cao, 2020; Wilson et al., 2020; Morawska et al., 2021; Tang et al., 2021). Several studies show that ventilation can reduce airborne infections by bringing fresh air to an occupied space and preventing infectious agents from accumulating indoors (Prather et al., 2020; Blocken et al., 2021; Park et al., 2021; Che et al., 2022; Motamedi et al., 2022; Xu et al., 2022). However, ventilation may not be enough to control airborne infection risk for densely occupied spaces or buildings without mechanical ventilation systems. In such cases, a layered approach should be combined to effectively minimize the airborne infection potential (Pei et al., 2021).

Ultraviolet germicidal irradiation (UVGI) is a disinfection technology that utilizes short-wavelength ultraviolet light to kill airborne microorganisms (Kowalski, 2010). It is applicable to all potential building system components where airborne microorganisms exist (Raeiszadeh and Adeli, 2020; Hou et al., 2021; Luo and Zhong, 2021; Srivastava et al., 2021). An upper-room UVGI system is a typical application where the UV fixture is installed near the room ceiling to irradiate a limited volume of the room along the ceiling to disinfect the air (Kowalski, 2010). Such a system divides the room into the upper UV radiation zone and the lower occupied zone.

The performance of an upper-room UVGI system varies with ventilation rate, UV fluence rate, and UV radiating volume (Beggs and Sleigh, 2002; Noakes et al., 2006; Park et al., 2022). Since virus disinfection takes place in the upper UVGI zone, the indoor airflow pattern also plays a crucial role in the disinfection performance of this system. Indoor airflow influences the residence time of viruses and aerosol dynamics in

* Corresponding author.
E-mail addresses: svp5982@psu.edu (S. Park), rgm1@psu.edu (R. Mistrick), wes25@psu.edu (W. Sitzabee), dxr51@psu.edu (D. Rim).

https://doi.org/10.1016/j.scitotenv.2023.165454
Received 20 November 2022; Received in revised form 22 June 2023; Accepted 8 July 2023
Available online 17 July 2023

the UVGI and occupied zones. Previous studies have emphasized the importance of a well-distributed airflow pattern in a room (Beggs and Sleigh, 2002; First et al., 2007; Whalen, 2009; Zhu et al., 2013; Pichurov et al., 2015; CDC, 2020). Specially, the buoyancy-driven upward airflow around occupants is directly related to the performance of upper-room UVGI systems because of its impact on transport of viral aerosols to the UVGI zone (First et al., 2007; Park et al., 2022). In this regard, previous studies have reported that the use of ceiling fans potentially increases both virus dispersion and virus removal in an occupied space (Zhu et al., 2013; Pichurov et al., 2015).

Indoor airflow pattern varies with building factors such as ventilation strategy, room size, room configuration, and indoor heat sources. Ventilation effectiveness is an indicator that quantifies the room airflow distribution performance. It indicates the quality of supply air distribution within a ventilated room, and the higher ventilation effectiveness represents the better removal of passive gaseous pollutants (Fisk et al., 1997; Novoselac and Srebric, 2003; Mundt et al., 2004; Rim and Novoselac, 2010). In general, a room with the buoyancy-driven airflow that results in air stratification and less air mixing (i.e., displacement ventilation) has a higher ventilation effectiveness than the well-mixed air condition (Rim and Novoselac, 2010; Ahn et al., 2018).

Although there have been studies on the effect of indoor airflow on upper-room UVGI systems, very few studies have examined the relationship between ventilation effectiveness and disinfection performance of upper-room UVGI systems. Given this background, the objective of this study is to examine the quantitative relationship between ventilation effectiveness and the UVGI disinfection performance for representative indoor conditions: 1) cooling with mixing ventilation, 2) cooling with displacement ventilation, and 3) all-air heating with mixing ventilation. Mixing ventilation is the most common building ventilation method for both cooling and heating conditions. Many mechanically ventilated buildings operate with the mixing ventilation system that provides supply air through ceiling diffusers (Amai and Novoselac, 2016). Displacement ventilation induces buoyancy-driven convective flow, which is also prevalent in occupied spaces without mechanical fan operating (Ji et al., 2007; Wang et al., 2014). This study investigated the impact of enhanced air mixing on the UVGI virus disinfection performance in those three airflow conditions. The results of this study and the proposed UVGI system modeling in the CFD simulation (in Supplementary data: Upper-room ultraviolet germicidal irradiation (UVGI) system modeling procedure) can help building designers and engineers apply upper-room UVGI systems effectively to densely occupied buildings such as classrooms, conference rooms, and hospitals.

2. Methods

2.1. Model geometry and boundary conditions

A computational fluid dynamics (CFD) simulation domain was designed based on a university classroom with a dimension of 7.62 m × 7.62 m × 3.05 m (length × width × height) (see Fig. 1). For mixing ventilation, four supply air diffusers (four-way type diffuser) and one exhaust opening were located at the ceiling, and each diffuser supplied the air jet angled at 30° to the ceiling surface (see Fig. S1). For the displacement ventilation, the low momentum air was supplied from the air inlet located on the wall (20 cm above from the floor), and the room air was exhausted at ceiling height. Two mixing fans with an area of 0.4 m × 0.4 m were applied between the UVGI and occupied zones while facing the wall to enhance the air mixing between the two zones (see Fig. 1 and Fig. S2).

The classroom model simulated nine students seated with a shoulder-to-shoulder distance of 2 m, based on the recommendation by the Centers for Disease Control and Prevention (CDC, 2020). The virus source could be a speaker or a student in the classroom. In this study, we pretested the disinfection performance of upper-room UVGI system with three source locations (see Fig. S3). Based on the preliminary result, the speaker was chosen as an infector in the simulation domain, given that the highest infection probability was observed with the speaker constantly emitting viral aerosols and a longer distance from the exhaust opening enabled more dispersion of viral aerosols in the room. The air jet speed from the speaker's mouth was set to 2 m/s with an air temperature of 34 °C and an opening size of 2 cm^2 based on the previous studies (Gupta et al., 2010; Ai and Melikov, 2018). The surface area of the human body was 1.8 m^2 and the metabolic heat generated by each occupant (55 W/m^2) was divided into 45% for the convective load and 55% for the radiative load (Rim et al., 2009; ASHRAE, 2017). The convective heat transfer rate was applied to the human surface as heat flux, while the radiative heat was evenly distributed to the surrounding walls, floor, and ceiling (Shan and Rim, 2018). The minimum required supply airflow rate based on ASHRAE standard 62.1 was set to 200 m^3/h with 100% outdoor air supply, which is equivalent to a ventilation rate of 1.1 h^{-1} for the classroom (ANSI/ASHRAE, 2019). The supply air temperatures were 14 °C for the mixing ventilation, 18 °C for the displacement ventilation, and 30 °C for all-air heating (Rim and Novoselac, 2010). The susceptibility constant of SARS-CoV-2 to UV-C was set to 3.77 × 10^{-3} $cm^2/\mu W \bullet s$ based on previous studies (Walker and Ko, 2007; Beggs and Avital, 2020).

For all-air heating, the internal heat loss through the exterior wall was considered (see Fig. 1a). The total heat loss rate for the classroom was calculated based on Eq. 1 (Ahn et al., 2018). The calculated heating load for 1.1 h^{-1}, 3 h^{-1}, and 5 h^{-1} were 38 W/m^2, 75 W/m^2, and 115 W/m^2, respectively.

$$q = \rho \times C_p \times Q \times (T_e - T_s) \quad (1)$$

where q is the total heat loss rate (W), ρ is the density of air (kg/m^3), C_p is the air specific heat ($J/kg \bullet K$), Q is the airflow rate (m^3/s), T_e is the temperature of the exhaust air (K), and T_s is the supply air temperature (K).

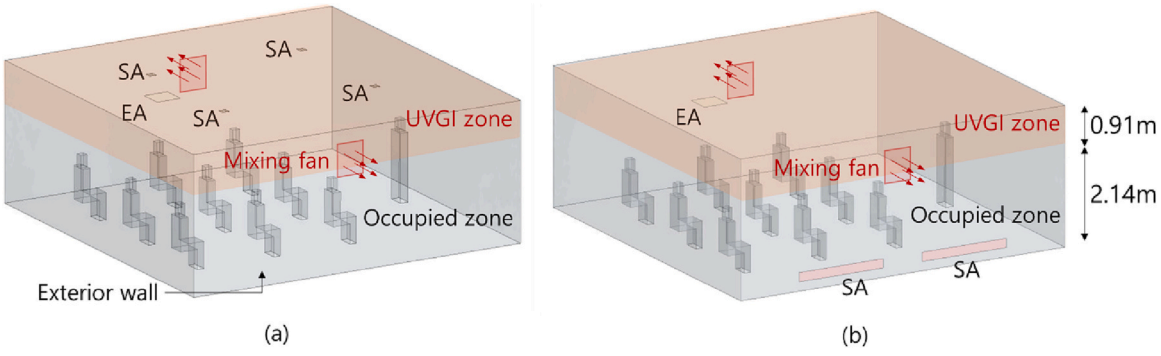

Fig. 1. The classroom configuration: a) mixing ventilation and all-air heating, b) displacement ventilation. Note that SA and EA represent supply air inlet and exhaust air outlet, respectively.

Considering the respiratory aerosol size range, viral aerosols size was set to 1 μm and 10 μm (Nicas et al., 2005; Zhang et al., 2015; Ai and Melikov, 2018). The viral aerosol emission rate from a speaker's mouth was 1.44 μg/h with a density of 1000 kg/m^3 (Pei et al., 2021). As particle deposition is one of the major indoor particle loss mechanisms along with ventilation, we set the deposition velocity for the floor as 0.003 cm/s for 1 μm particles and 0.3 cm/s for 10 μm particles (Lai and Nazaroff, 2000).

The upper-room UVGI system utilized in this study consisted of four wall-mounted fixtures (PL-L36WTUV lamps), with a single unit centered along each of the room walls and mounted at 2.44 m above the floor (see Fig. S4). The 254 nm UV radiation consisted of 670 mW per fixture that contained two 36 W compact fluorescent lamps and produced a wide flat beam directed along and just above the horizontal plane. Laboratory photometric measurements of the emitted distribution were applied in the Visual Software* (https://www.acuitybrands.com/resources/technical-resources/visual-lighting-software) to compute the spatial distribution of the fluence rate across the upper UVGI zone. The fluence rate is a measure of the total radiant power incident from all directions through an infinitesimally small sphere of cross-sectional area dA. Three different calculation planes were applied to compute the fluence rate at points through the center of three different horizontal slices through the upper UVGI zone (see Fig. S5). The UV fluence rates from these calculations were then applied to interpolate values within each cell of the CFD simulation at its corresponding position.

2.2. CFD simulation

The virus disinfection associated with the upper room UVGI system was simulated using a commercial CFD software, STAR-CCM+ version 2021.03. CFD model has been widely used as a reliable tool to simulate the airborne transmission (Sheikhnejad et al., 2022). In the present study, a Eulerian two-phase model was employed to simulate the viral aerosol transport in indoor air, while the UV disinfection process was coupled in the transport equation as follows (Zhu et al., 2013):

$$\frac{\partial C}{\partial t}+\frac{\partial}{\partial x_j}\left(Cu_j\right)=\frac{\partial}{\partial x_j}\left(\left(D+D_t\right)\frac{\partial C}{\partial x_j}\right)-KIC \tag{2}$$

where, C is the particle concentration (μg/m^3), u_j is the velocity component (m/s), D is the molecular diffusion coefficient (m^2/s), D_t is the kinematic diffusion coefficient (m^2/s), K is the susceptibility constant (cm^2/(μW•h)), and I is UV fluence rate (μW/cm^2).

The total virus removal rate of upper-room UVGI systems is determined by ventilation rate, a (h^{-1}) and UVGI factors, KIV_{UV} (h^{-1}) (K: the susceptibility constant of virus, I: UV fluence rate, and V_{UV}: the UV radiating volume ratio) (Park et al., 2022; Zhu et al., 2022). In this study, the virus removal rate of UVGI factor was estimated as 102 h^{-1} (K :25.11 μW/cm^2, I: 3.77 × 10^{-3} cm^2/μW-s, and V_{UV}: 0.3), which is about 90 times higher than that of ventilation when the ventilation rate is 1.1 h^{-1}.

We used the Reynolds Averaged Navier-Stokes (RANS) model with the Shear Stress Transport (SST) k-ω model to simulate the transport of viral aerosols under the effect of the buoyancy-driven convective thermal plume developed from the occupants (Menter, 1994; Pei and Rim, 2021).

The detailed CFD simulation procedure process as well as the modeling procedure of UV fluence field were developed based the previous study (Park et al., 2022), which is described in Supplementary data: Upper-room ultraviolet germicidal irradiation (UVGI) system modeling procedure.

2.3. Mesh generation and verification of CFD simulation

For the mesh generation of the simulation domain, polyhedral mesh was employed because of its advantage that gradients can be well approximated (Sosnowski et al., 2018). The base cell size was set to 15 cm, with the first cell size of the human surface of 5 mm and a surface growth rate of 1.2, which resulted in the average y+ value (dimensionless wall) of 3.7. The cell sizes near the occupants and the supply/exhaust air openings were also refined (the first cell size of 5 mm) to improve the estimation accuracy of heat and mass transfer rates (see Fig. S6). Before simulating a densely occupied classroom, we compared the measured and simulated results of spatial non-uniform distributions of air velocity and particle concentrations to ensure the reliability of the modeling approach. The details are described in Supplementary data: The validation of the airflow field.

A grid sensitivity analysis was performed to ensure the quality and consistency of the CFD simulation results based on the method used in the previous studies (Pei et al., 2021; Park et al., 2022). Three grid resolutions, 195,000, 294,000, and 663,000, were tested, while ASHRAE breathing zone concentrations were compared with and without UVGI operation. The result shows that the grid resolution of 195,000 yielded a 25% higher concentration than the 663,000 grid, whereas the concentration difference between 294,000 and 663,000 grids was up to 9% for UVGI operating condition. This suggests that the grid resolution of 294,000 can generate a converged solution for the particle transport model with UVGI operation. Table S1 provides the details of the grid sensitivity analysis.

The mass and energy balances in the simulation domain were double-checked to verify the simulation results. The difference between supply and exhaust air flow rate was <0.01%, and the difference between total heat gain and total heat loss in the domain was <0.09%. Furthermore, the room average viral aerosol concentration from the CFD simulations was compared with that of the well-mixed mass balance model as follows (Kim et al., 2019):

$$C_{ss}=\frac{E}{(a+\beta)V} \tag{3}$$

where C_{ss} is the steady-state indoor concentration (μg/m^3), E is the emission rate (μg/h), a is ventilation rate (h^{-1}), β is the deposition rate (h^{-1}), and V is the total room volume (m^3). Note that the outdoor concentration is not considered because the speaker is the only viral aerosol source.

In addition, CFD results were compared with the mass balance model for the quality control of CFD simulations. The concentration differences between the mass balance model and CFD simulations were <10% for all ventilation strategies with three ventilation rates and two particle sizes (see Fig. S7).

2.4. Calculation of ventilation effectiveness and performance of the upper-room UVGI system

The first step to estimate ventilation effectiveness is to calculate the age-of-air distribution in the room. In the CFD simulation, a tracer gas, SF_6, was released constantly in each cell of the simulation domain with an emission rate of 1.0 × 10^{-6} kg/m^3•s. Note that age-of-air (τ) at a given location was calculated based on local tracer gas concentrations and ventilation rate as follows:

$$\tau=C_i/(C_e\times a) \tag{4}$$

where C_i is SF_6 mole fraction at a local point I (dimensionless) C_e is SF_6 mole fraction at the room exhaust (dimensionless), and a is the ventilation rate of the room (h^{-1}).

Ventilation effectiveness (VE) for a specific zone of interest is defined as the ratio of age-of-air at the exhaust to age-of-air of the point of interest as follows (Nielsen, 1993):

$$\mathrm{VE}=\frac{\tau_e}{\tau_i} \tag{5}$$

where τ_e is age of air at the room exhaust (h) and τ_i is age of air at the

point I (h).

Along with ventilation effectiveness, disinfection effectiveness (DE) was defined as the ratio of the reduced room-average viral aerosol concentration with the operation of the UVGI system to the room-average viral aerosol concentration without the UVGI system operation, as shown in Eq. 6.

$$DE = 1 - \frac{C_{on}}{C_{off}} \quad (6)$$

where C_{on} is the viral aerosol concentration when the UVGI system is operating (μg/m^3) and C_{off} is the viral aerosol concentration when the UVGI system is not operating (μg/m^3).

In addition to ventilation effectiveness and disinfection effectiveness, the recirculation airflow (RA) was calculated using Eq. 7. It represents the airflow rate between the upper UVGI and occupied zones which substantially influences the virus disinfection performance of upper-room UVGI system (Beggs and Sleigh, 2002)

$$RA = 0.5(L \times W)v_{int} \quad (7)$$

where, l is the length of room (m), W is the width of the room (m), and v_{int} is the area-averaged air speed across the boundary between the upper UVGI and occupied zones (m/s).

2.5. Simulation matrix for the study of ventilation effectiveness and disinfection effectiveness

Table 1 summarizes a total of 15 simulation cases to investigate how the relationship between ventilation effectiveness and disinfection effectiveness varies with ventilation strategy, ventilation rate, and indoor air mixing condition. Three ventilation strategies (cooling with mixing ventilation, cooling with displacement ventilation, and all-air heating with mixing ventilation) along with two mixing fan airspeeds (0.83 m/s and 1.44 m/s) were simulated with three ventilation rates (1.1 h^{-1}, 3 h^{-1}, and 5 h^{-1}) for the classroom (Zhu et al., 2013; Pichurov et al., 2015). Note that the mixing fans were only applied to the case with a ventilation rate of 1.1 h^{-1}, which is the minimum ventilation rate required by ASHRAE standard 62.1 (ANSI/ASHRAE, 2019), as the higher ventilation rates of 3 h^{-1} and 5 h^{-1} yield relatively larger mixing effects without mixing fans (Heiselberg, 1996).

Table S2 shows the summary of all CFD simulation results. For each simulation case, the viral aerosol concentrations were calculated for the ASHRAE breathing zone, defined as the air volume ranging from 7.55 cm to 180 cm above the floor and 60 cm away from the walls (ANSI/ASHRAE, 2019). The average breathing zone concentration was estimated using 200 evenly distributed monitoring points in the CFD model and normalized by the emission concentration.

Table 1
The summary of simulation scenarios.

Case ID	Ventilation strategy	Ventilation rate (h^{-1})	Fan operation
M1	Mixing	1.1	No
M2	Mixing	1.1	Airspeed: 0.83 m/s
M3	Mixing	1.1	Airspeed: 1.44 m/s
M4	Mixing	3	No
M5	Mixing	5	No
D1	Displacement	1.1	No
D2	Displacement	1.1	Airspeed: 0.83 m/s
D3	Displacement	1.1	Airspeed: 1.44 m/s
D4	Displacement	3	No
D5	Displacement	5	No
H1	All-air heating	1.1	No
H2	All-air heating	1.1	Airspeed: 0.83 m/s
H3	All-air heating	1.1	Airspeed: 1.44 m/s
H4	All-air heating	3	No
H5	All-air heating	5	No

3. Results and discussion

3.1. Indoor airflow distribution

Table 2 summarizes the steady-state CFD simulation results of age-of-air, ventilation effectiveness, the room air speed, and recirculation airflow rate for the classroom with ten occupants. According to the result, the mixing ventilation consistently shows a higher average room air speed (0.10 m/s–0.12 m/s) than displacement ventilation (0.06 m/s–0.10 m/s) and all-air heating (0.05 m/s–0.11 m/s). For all cases considered, ventilation effectiveness of the mixing ventilation is close to one (0.98–1.04), which means that the mixing ventilation yields an airflow distribution close to uniform air mixing even at the ASHARE minimum ventilation rate. Displacement ventilation without any additional air mixing shows a relatively higher ventilation effectiveness range of 1.13–1.20 (Cases D1, D4, and D5), which means more fresher air (i.e., lower age-of-air) supplied to the breathing zone than mixing ventilation. This pattern was also reported by other studies (Gan, 1995; Lin et al., 2005; Ahn et al., 2018). In such condition, vertical air stratification occurs, generating a relatively high gradient of age-of-air, which results in a high standard deviation of age-of-air and the viral aerosol concentration (see Table 2 and Table S2). All-air heating yields the lowest ventilation effectiveness among the three ventilation strategies, mainly because the warm air from the ceiling diffusers does not fully reach the lower part of the room. This condition leads to short-circuiting of airflow near the ceiling and relatively poor ventilation performance (Novoselac and Srebric, 2003; Rim and Novoselac, 2010).

Fig. 2 shows the viral aerosol concentration distribution with three ventilation rates of 1.1 h^{-1}, 3 h^{-1}, and 5 h^{-1} under three ventilation strategies for an aerosol size of 1 μm. In this figure, the air jet from the speaker's mouth is disrupted right after emission under mixing ventilation because of a relatively higher air speed and mixing effect (ventilation effectiveness is 1.00–1.01) for all ventilation rates. Meanwhile, the air jet travels a longer distance under displacement ventilation (ventilation effectiveness is 1.13–1.20) and all-air heating (ventilation effectiveness is 0.70–0.86) even with about five times increase in ventilation rate from 1.1 h^{-1} to 5 h^{-1}. This result reveals that mixing ventilation yields relatively uniform concentrations even at the minimum ventilation rate based on ASHRAE 62.1 (1.1 h^{-1}), implying that all occupants have relatively similar infection risks under mixing ventilation. On the other hand, with less air mixing under displacement ventilation and all-air heating, occupants close to an infector are more prone to be exposed to a high concentration and have a higher infection risk (Pei et al., 2021).

3.2. Effect of the mixing fan operation on ventilation effectiveness and disinfection effectiveness of a UVGI system

Fig. 3 illustrates spatial age-of-air distributions of three ventilation strategies depending on mixing fan operating condition at the minimum ventilation rate of 1.1 h^{-1}. Age-of-air distributions are fairly even for mixing ventilation regardless of the mixing fan operation, suggesting a marginal effect of mixing fan operation on spatial age-of-air distributions. In this case, ventilation effectiveness is close to one (0.98–1.04) (see Table 2). Displacement ventilation shows a relatively low age-of-air compared to the other two ventilation strategies because the fresh air supplied at floor level is exhausted before mixing with indoor air due to the vertically stratified air. And the vertical age-of-air difference within a room decreases when the mixing fans are operating. Note that such stratified airflow also occurs in occupied buildings where mechanical ventilation does not exist and outdoor infiltrated air is mainly driven by indoor heat sources. Regarding all-air heating, it has the highest range of age-of-air (i.e., poorly ventilated stagnant air) near occupants compared to the other two ventilation strategies because of the bypassing of the supply air directly to the exhaust. When the mixing fans are operating, ventilation effectiveness decreases from 1.13 to 1.03 for the

Table 2
Summary of age-of-air, ventilation effectiveness, room air speed, and recirculation airflow rate.

Case ID	Age-of-air		Ventilation effectiveness		Room air speed (m/s)		Recirculation airflow rate (m^3/h)
	Average	SD	Average	SD	Average	SD	
1M	0.91	0.03	1.00	0.03	0.11	0.04	5999
2M	0.87	0.02	1.04	0.03	0.12	0.05	6100
3M	0.90	0.01	1.01	0.02	0.12	0.08	5722
4M	0.34	0.01	0.98	0.03	0.10	0.07	6150
5M	0.20	0.01	1.00	0.03	0.12	0.11	8164
1D	0.80	0.10	1.13	0.10	0.06	0.03	2940
2D	0.84	0.09	1.08	0.08	0.07	0.05	3450
3D	0.88	0.08	1.03	0.08	0.10	0.08	4625
4D	0.28	0.07	1.18	0.04	0.06	0.03	3046
5D	0.17	0.01	1.20	0.03	0.06	0.04	3812
1H	1.30	0.03	0.70	0.02	0.05	0.04	2570
2H	1.18	0.02	0.77	0.01	0.07	0.05	2820
3H	1.10	0.02	0.83	0.01	0.09	0.08	4100
4H	0.43	0.03	0.78	0.06	0.07	0.07	3006
5H	0.23	0.01	0.86	0.06	0.10	0.11	5060

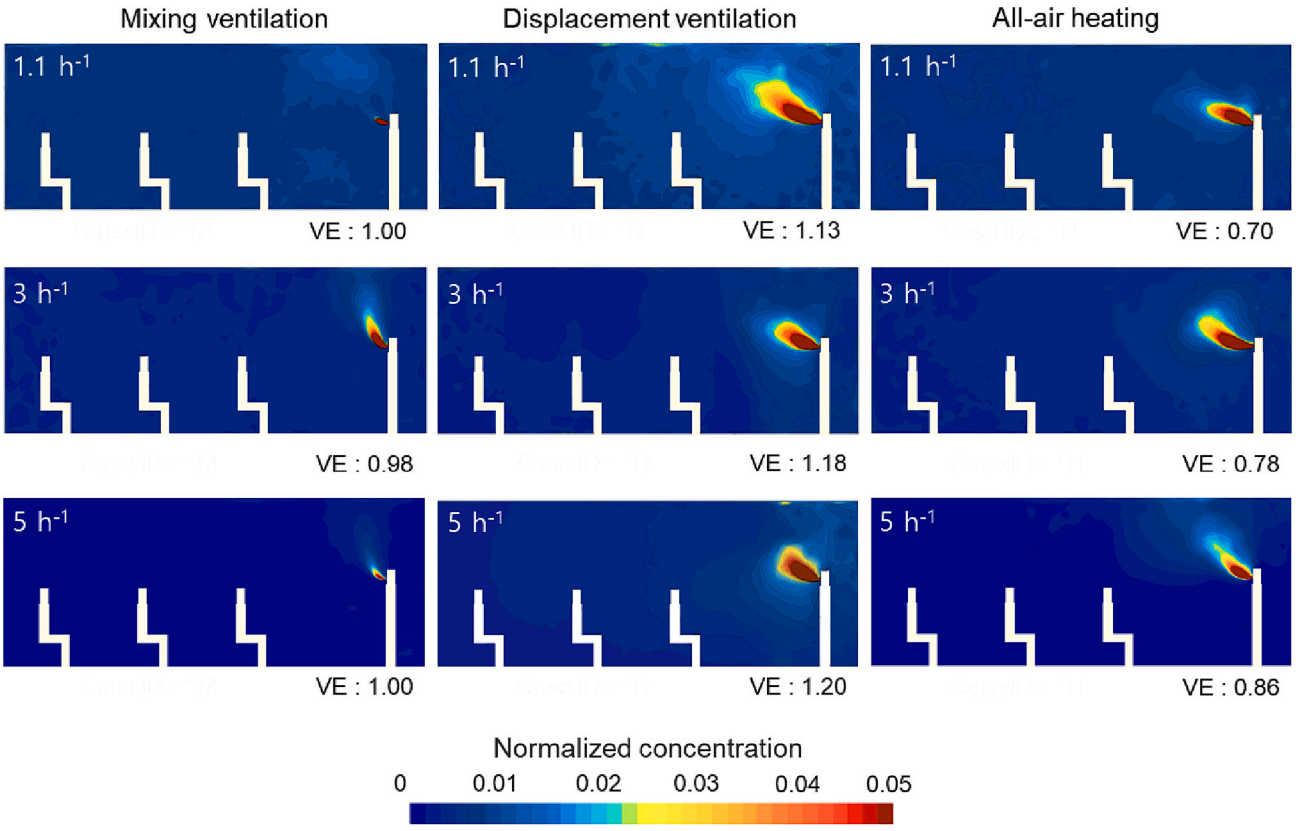

Fig. 2. Viral aerosol concentration distributions under three ventilation rates (1 h^{-1}, 3 h^{-1}, and 5 h^{-1}) for mixing ventilation, displacement ventilation, and all-air heating. Note that the viral aerosol size is 1 μm and the concentration is normalized by the emission concentration.

displacement ventilation while it increases from 0.70 to 0.83 for all-air heating. Note that the enhanced air mixing disrupts the air jet from the infector (see Figs. S8 and S9).

Fig. 4 illustrates the disinfection effectiveness of the UVGI system and the recirculation airflow rate depending on the mixing fan operating conditions. The recirculation airflow represents the airflow rate between the upper UV radiation zone and the occupied zone (Beggs and Sleigh, 2002). Since the higher recirculation airflow can deliver more viral aerosols to the UVGI zone, it plays a vital role in the virus disinfection performance of upper-room UVGI system (Noakes et al., 2004).

According to Fig. 4, mixing ventilation shows higher disinfection effectiveness of 0.91–0.98 than the other two ventilation strategies at a ventilation rate of 1.1 h^{-1}. The recirculation airflow rate ranges from 5720 m^3/h to 6100 m^3/h. And as shown in Table 2 and Fig. 3, since the mixing fan does not significantly influence the spatial age-of-air distribution, the mixing fan operation has marginal effects on disinfection effectiveness and recirculation airflow rate. In contrast, under displacement ventilation, as the mixing fan operates with a higher mixing fan airspeed, ventilation effectiveness decreases from 1.13 to 1.03 and the recirculation airflow rate notably increases from 2940 m^3/h to 4625 m^3/h (see Table 2). This change leads to about 10% increase in the virus disinfection effectiveness for the two aerosol sizes. A similar trend appears to occur during the heating season. For all-air heating, the mixing fan operation leads to an increase in ventilation effectiveness (from 0.70 to 0.83) and recirculation airflow rate (from 2570 m^3/h to 4100 m^3/h), which results in up to 13% increases in the disinfection

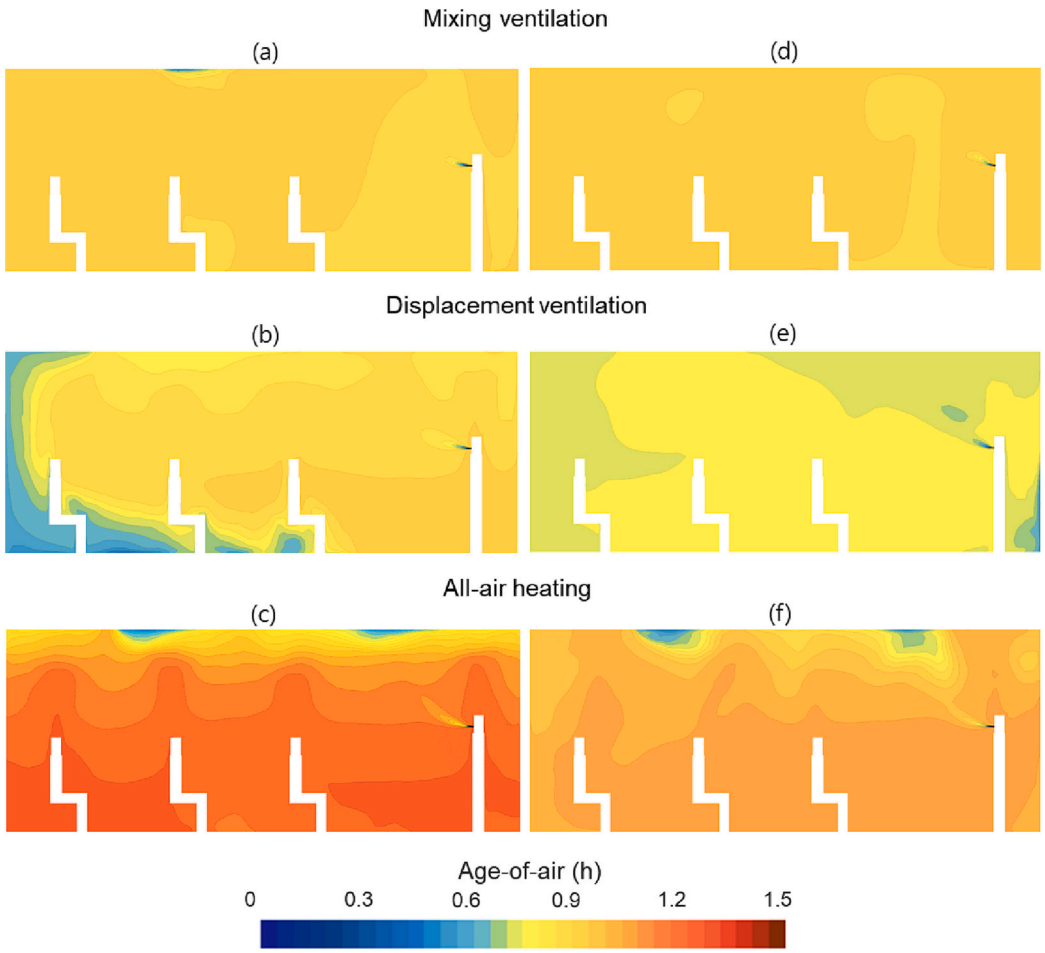

Fig. 3. The distribution of age-of-air under three ventilation strategies and the mixing fan operating condition: a, b, c) mixing fan is off, d, e, f) mixing fans are operating with an airspeed of 1.44 m/s.

effectiveness. These results imply that enhancing indoor air mixing can contribute to improving UVGI disinfection performance for cooling with displacement ventilation and all-air heating conditions. This finding also supports previous studies that the ceiling fan can be an effective measure to improve the performance of an upper-room UVGI system by increasing the diffusivity of virus (Zhu et al., 2013; Pichurov et al., 2015; Rudnick et al., 2015; Zhu et al., 2022). However, previous studies noted that too high fan airspeed is likely to decrease the residence time of viral aerosols in the UVGI zone; therefore, the mixing fan speed and airflow direction should be determined considering the virus disinfection process in the upper-room UVGI system.

3.3. Relationship between ventilation effectiveness and disinfection effectiveness of a UVGI system

Fig. 5 shows the relationship between ventilation effectiveness and disinfection effectiveness for a UVGI system with a viral aerosol size of 1 μm and 10 μm for the total 15 cases considered. Different symbol colors, sizes, and shapes represent the mixing fan operating condition, ventilation rate, and ventilation strategy, respectively. These three factors influence the ventilation effectiveness on the x-axis. Note that disinfection effectiveness on the y-axis is based on the average viral aerosol concentration of the ASHRAE breathing zone.

Fig. 5 depicts that disinfection effectiveness ranges from 0.87 to 0.99 for 1 μm particles and from 0.75 to 0.94 for 10 μm particles. The disinfection effectiveness for 10 μm particles is lower than that for 1 μm particles, mainly because the downward force of gravity is proportional to the particle mass and 10 μm aerosols settle on indoor surfaces more quickly. This trend implies that a higher ventilation effectiveness does not necessarily yield a high removal of large particles (>7 μm viral aerosol) that carry more virus load than 1 μm particles (Rim and Novoselac, 2010; Mao et al., 2020; Zhou and Zou, 2021).

The previous section (see Section 3.2 Effect of the mixing fan operation on ventilation effectiveness and disinfection effectiveness of a UVGI system) discussed that the virus disinfection by a UVGI system is maximized as indoor air is well-mixed, as Fig. 5a and b clearly show that trend. This result provides a quantitative explanation on the previous studies that well-distributed airflow is likely to increase the chance for viral aerosols to be exposed to the upper UVGI zone (Noakes et al., 2004; Noakes et al., 2006; Zhu et al., 2013; Pichurov et al., 2015).

In general, it has been reported that displacement ventilation yields a higher ventilation effectiveness and provides good indoor air quality due to the vertical air stratification that supplies fresher air to the human breathing zone (Brohus and Nielsen, 1996; Lin et al., 2005; Tian et al., 2010; Norbäck et al., 2011). Some recent studies have pointed out that displacement ventilation is a better way to mitigate airborne transmission than mixing ventilation in conventional indoor environments (Liu et al., 2022; Nair et al., 2022; Ren et al., 2022; Su et al., 2022). On the other hand, other studies have reported that without air mixing, the air jet from a speaker's mouth can travel a longer distance, which increases infection risk near infectors under displacement ventilation (Lin et al., 2012; Pei et al., 2021). However, mixing ventilation could lower the infection risk even with a short social distancing between occupants smaller than 1.5 m (Li et al., 2021). According to the results presented in this study, the virus disinfection of an upper-room UVGI system is enhanced with a well-mixed airflow pattern and the benefit of UVGI

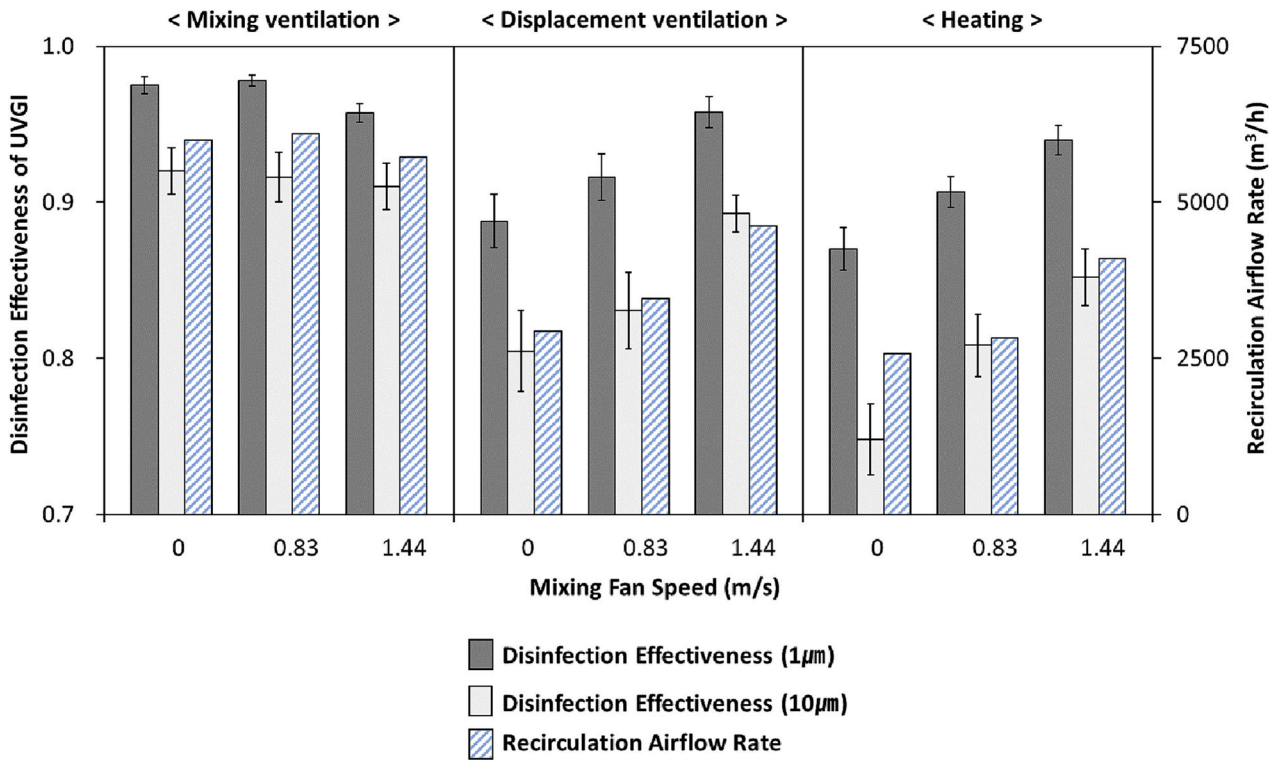

Fig. 4. Disinfection effectiveness of a UVGI system and the recirculation airflow rate with different mixing fan operating conditions when the ventilation rate is 1.1 h^{-1}. The error bars represent the standard error.

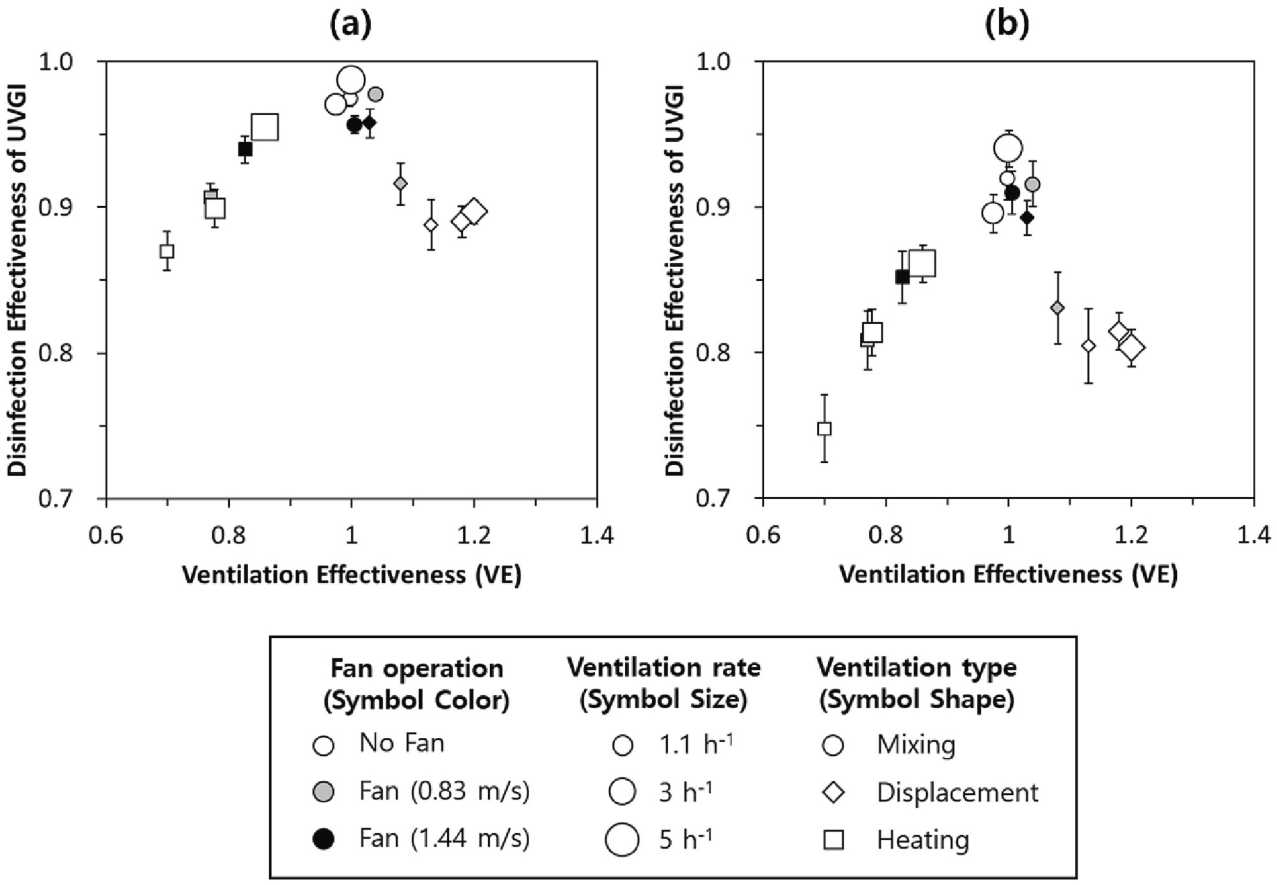

Fig. 5. Ventilation effectiveness vs. disinfection effectiveness of a UVGI system for (a) 1 μm and (b) 10 μm size aerosols. Note that the error bars represent the standard error and the disinfection effectiveness was calculated using the ASHRAE breathing zone concentration.

system can be maximized with increasing air recirculation in the room (see Table S2).

Note that positive correlations between the recirculation airflow rate and UVGI disinfection effectiveness was observed for both 1 μm and 10 μm aerosols with R^2 values >0.85 (see Fig. S11). The figure reveals that 1) the recirculation airflow rate increases with ventilation rate, 2) mixing ventilation has a higher recirculation airflow rate than the other two ventilation strategies, and 3) operating air mixing fans increases in the recirculation airflow rate, especially for displacement ventilation and all-air heating. Finally, Fig. 6 shows the positive correlation between the room air speed and disinfection effectiveness of UVGI system. According to the figure, UVGI disinfection effectiveness increases notably with the average room air speed, especially for larger viral aerosols (i.e.,10 μm) with the average room air speed >0.1 m/s. These results imply that in both cooling and heating seasons, enhancing air recirculation across the UVGI and occupied zones are desired as it can help improve the performance of an upper-room UVGI system.

3.4. Study implications and limitations

Based on our analysis, upper-room UVGI system could be an effective measure to mitigate the infection risk for densely occupied spaces because of its large disinfection effect compared to increasing ventilation rate (Srivastava et al., 2021; Park et al., 2022; Karam et al., 2023). For an occupied room with mixing ventilation, an upper-room UVGI system can yield >90% virus disinfection effect for 1 μm–10 μm size aerosols due to the air mixing effect. However, during winter season when the airborne virus infection risk can be high (Mallapaty, 2020), short air circuiting problem can occur (Rim and Novoselac, 2009; Rim and Novoselac, 2010). In such case, additional measures to increase indoor air mixing or ventilation is desired. Meanwhile, for indoor spaces where the buoyancy-driven convective airflow is prevalent (i.e., displacement ventilation or no mechanical ventilation systems such as portable classrooms), the role of air mixing in improving the UVGI performance is highlighted. In general, naturally ventilated rooms have a buoyancy-driven airflow pattern similar to the room airflow created by displacement ventilation (Ji et al., 2007; Wang et al., 2014). In this case, operating mixing fans in the occupied space can help improve the virus disinfection effectiveness of a UVGI system.

A few limitations of this study should be noted. While the major focus of this study is virus disinfection performance depending on indoor ventilation and air mixing strategy, future studies should examine potential secondary contaminant generations from UVGI systems. This study assumes a constant virus death rate and an UV radiating volume of 30% of the total room volume. Future studies are warranted to investigate the combined effects of variations of virus death rate and UVGI volume on the disinfection performance in different indoor environments (e.g., classrooms, conference rooms, and hospital waiting rooms).

4. Conclusions

The present study evaluated the effects of the room airflow pattern and ventilation strategy on the disinfection performance of upper-room UVGI system. The results show that at the minimum required ventilation rate of 1.1 h−1, enhanced air mixing notably improves the UVGI disinfection performance for displacement ventilation and all-air heating condition, while operating mixing fans has a marginal effect for mixing ventilation. Furthermore, disinfection effectiveness is positively correlated with the room average air speed, suggesting that >90% disinfection effects for 1 μm–10 μm size aerosols with increased air recirculation and the room average air speed >0.1 m/s. The results of the present study can provide engineers and researchers insights into the application of upper-room UVGI system, especially for occupied spaces with minimum air mixing (e.g., rooms with displacement ventilation at

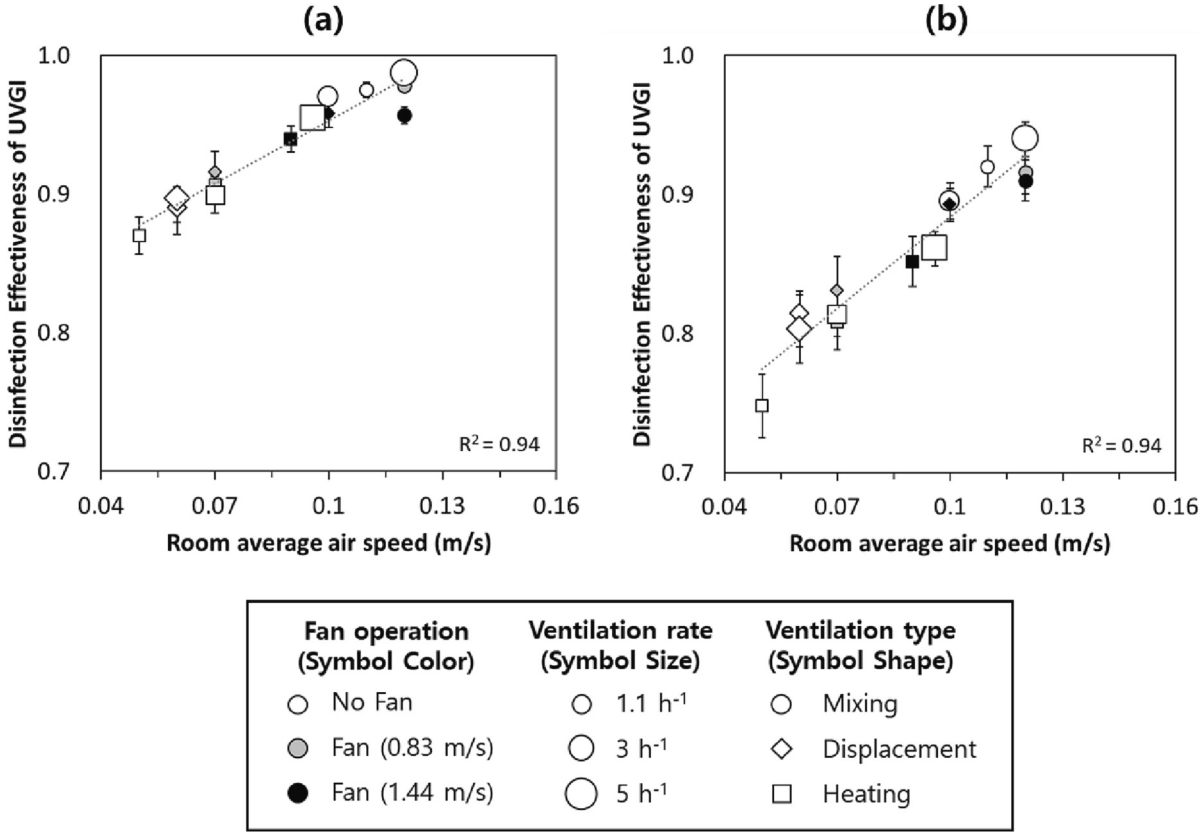

Fig. 6. Disinfection effectiveness of a UVGI system vs. the room average air speed for (a) 1 μm and (b) 10 μm aerosols. Note that the error bars represent the standard error and the disinfection effectiveness was calculated using the ASHRAE breathing zone concentration.

small ventilation rates or with all air heating).

Declaration of competing interest

The authors declare that they have no known competing financial interests or personal relationships that could have appeared to influence the work reported in this paper.

Data availability

Data will be made available on request.

Acknowledgments

The research presented in this paper was supported by the by the U.S. National Science Foundation (NSF Grant 1944325) as well as the Penn State Office of Physical Plant.

Appendix A. Supplementary data

Supplementary data to this article can be found online at https://doi.org/10.1016/j.scitotenv.2023.165454.

References

Ahn, H., Rim, D., Lo, L.J., 2018. Ventilation and energy performance of partitioned indoor spaces under mixing and displacement ventilation. Build. Simul. 11, 561–574. https://doi.org/10.1007/s12273-017-0410-z.

Ai, Z.T., Melikov, A.K., 2018. Airborne spread of expiratory droplet nuclei between the occupants of indoor environments: a review. Indoor Air 28 (4), 500–524. https://doi.org/10.1111/ina.12465.

Amai, H., Novoselac, A., 2016. Experimental study on air change effectiveness in mixing ventilation. Build. Environ. 109, 101–111. https://doi.org/10.1016/j.buildenv.2016.09.015.

ANSI/ASHRAE, 2019. Standard 62.1-2019 Ventilation for Acceptable Indoor Air Quality. American Society of Heating, Refrigerating and Air-Conditioning Engineers.

ASHRAE, 2017. Fundamentals, Chapter 18: Nonresidential Cooling and Heating Load Calculations. American Society of Heating, Refrigerating and Air Conditioning Engineers, Atlanta.

Beggs, C.B., Avital, E.J., 2020. Upper-room ultraviolet air disinfection might help to reduce COVID-19 transmission in buildings: a feasibility study. Peer J. 8, e10196 https://doi.org/10.7717/peerj.10196.

Beggs, C.B., Sleigh, P.A., 2002. A quantitative method for evaluating the germicidal effect of upper room UV fields. J. Aerosol Sci. 33 (12), 1681–1699. https://doi.org/10.1016/S0021-8502(02)00117-9.

Blocken, B., van Druenen, T., Ricci, A., Kang, L., van Hooff, T., Qin, P., Brombacher, A.C., 2021. Ventilation and air cleaning to limit aerosol particle concentrations in a gym during the COVID-19 pandemic. Build. Environ. 193, 107659 https://doi.org/10.1016/j.buildenv.2021.107659.

Brohus, H., Nielsen, P.V., 1996. Personal exposure in displacement ventilated rooms. Indoor Air 6 (3), 157–167. https://doi.org/10.1111/j.1600-0668.1996.t01-1-00003.x.

CDC, 2020. How COVID-19 Spreads? US Centers for Disease Control and Prevention (Accessed January 2, 2021). https://www.cdc.gov/corona/2019-ncov/prevent-getting-sick/how-covid-spreads.html.

Che, W., Ding, J., Li, L., 2022. Airflow deflectors of external windows to induce ventilation: towards COVID-19 prevention and control. Sustain. Cities Soc. 77, 103548 https://doi.org/10.1016/j.scs.2021.103548.

First, M., Rudnick, S.N., Banahan, K.F., Vincent, R.L., Brickner, P.W., 2007. Fundamental factors affecting upper-room ultraviolet germicidal irradiation—part I. Experimental. J. Occup. Environ. Hyg. 4 (5), 321–331. https://doi.org/10.1080/15459620701271693.

Fisk, W.J., Faulkner, D., Sullivan, D., Bauman, F., 1997. Air change effectiveness and pollutant removal efficiency during adverse mixing conditions. Indoor Air 7 (1), 55–63. https://doi.org/10.1111/j.1600-0668.1997.t01-3-00007.x.

Gan, G., 1995. Evaluation of room air distribution systems using computational fluid dynamics. Energy Build. 23 (2), 83–93. https://doi.org/10.1016/0378-7788(95)00931-0.

Gupta, J.K., Lin, C.H., Chen, Q., 2010. Characterizing exhaled airflow from breathing and talking. Indoor Air 20 (1), 31–39. https://doi.org/10.1111/j.1600-0668.2009.00623.x.

Heiselberg, P., 1996. Room air and contaminant distribution in mixed ventilation. ASHRAE Trans. 102 (2), 332–339.

Hou, M., Pantelic, J., Aviv, D., 2021. Spatial analysis of the impact of UVGI technology in occupied rooms using ray-tracing simulation. Indoor Air 31 (5), 1625–1638. https://doi.org/10.1111/ina.12827.

Ji, Y., Cook, M.J., Hanby, V., 2007. CFD modelling of natural displacement ventilation in an enclosure connected to an atrium. Build. Environ. 42 (3), 1158–1172. https://doi.org/10.1016/j.buildenv.2005.11.002.

Karam, J., Ghali, K., Ghaddar, N., 2023. Pulsating jet ventilation add-ons performance for reducing the contaminant spread in classrooms: portable air cleaners vs. upper room UVGI. Build. Environ. 229, 109946 https://doi.org/10.1016/j.buildenv.2022.109946.

Kim, J., Park, S., Kim, H., Yeo, M.S., 2019. Emission characterization of size-resolved particles in a pre-school classroom in relation to children's activities. Indoor Built Environ. 28 (5), 659–676. https://doi.org/10.1177/1420326X17707565.

Kowalski, W.J., 2010. Ultraviolet Germicidal Irradiation Handbook: UVGI for Air and Surface Disinfection. Springer-Verlag, New York, NY.

Lai, A.C., Nazaroff, W.W., 2000. Modeling indoor particle deposition from turbulent flow onto smooth surfaces. J. Aerosol Sci. 31 (4), 463–476. https://doi.org/10.1016/S0021-8502(99)00536-4.

Li, W., Chong, A., Hasama, T., Xu, L., Lasternas, B., Tham, K.W., Lam, K.P., 2021. Effects of ceiling fans on airborne transmission in an air-conditioned space. Build. Environ. 198, 107887 https://doi.org/10.1016/j.buildenv.2021.107887.

Lin, Z., Chow, T.T., Fong, K.F., Tsang, C.F., Wang, Q., 2005. Comparison of performances of displacement and mixing ventilations. Part II: indoor air quality. Int. J. Refrig. 28 (2), 288–305. https://doi.org/10.1016/j.ijrefrig.2004.04.006.

Lin, Z., Wang, J., Yao, T., Chow, T.T., 2012. Investigation into anti-airborne infection performance of stratum ventilation. Build. Environ. 54, 29–38. https://doi.org/10.1016/j.buildenv.2012.01.017.

Liu, S., Koupriyanov, M., Paskaruk, D., Fediuk, G., Chen, Q., 2022. Investigation of airborne particle exposure in an office with mixing and displacement ventilation. Sustain. Cities Soc. 79, 103718 https://doi.org/10.1016/j.scs.2022.103718.

Luo, H., Zhong, L., 2021. Ultraviolet germicidal irradiation (UVGI) for in-duct airborne bioaerosol disinfection: review and analysis of design factors. Build. Environ. 197, 107852 https://doi.org/10.1016/j.buildenv.2021.107852.

Mallapaty, S., 2020. Why COVID outbreaks look set to worsen this winter. Nature 586 (7831), 653–654. https://link.gale.com/apps/doc/A639696125/AONE?u=anon~9c8880c1&sid=googleScholar&xid=6109ba0f.

Mao, N., An, C.K., Guo, L.Y., Wang, M., Guo, L., Guo, S.R., Long, E.S., 2020. Transmission risk of infectious droplets in physical spreading process at different times: a review. Build. Environ. 185, 107307 https://doi.org/10.1016/j.buildenv.2020.107307.

Menter, F.R., 1994. Two-equation eddy-viscosity turbulence models for engineering applications. AIAA J. 32 (8), 1598–1605.

Morawska, L., Cao, J., 2020. Airborne transmission of SARS-CoV-2: the world should face the reality. Environ. Int. 139, 105730 https://doi.org/10.1016/j.envint.2020.105730.

Morawska, L., Milton, D.K., 2020. It is time to address airborne transmission of coronavirus disease 2019 (COVID-19). Clin. Infect. Dis. 71 (9), 2311–2313. https://doi.org/10.1093/cid/ciaa939.

Morawska, L., Allen, J., Bahnfleth, W., Bluyssen, P.M., Boerstra, A., Buonanno, G., Yao, M., 2021. A paradigm shift to combat indoor respiratory infection. Science 372 (6543), 689–691. https://doi.org/10.1126/science.abg2025.

Motamedi, H., Shirzadi, M., Tominaga, Y., Mirzaei, P.A., 2022. CFD modeling of airborne pathogen transmission of COVID-19 in confined spaces under different ventilation strategies. Sustain. Cities Soc. 76, 103397 https://doi.org/10.1016/j.scs.2021.103397.

Mundt, E., Mathisen, H.M., Nielsen, P.V., Moser, A., 2004. Ventilation Effectiveness. Rehva.

Nair, A.N., Anand, P., George, A., Mondal, N., 2022. A review of strategies and their effectiveness in reducing indoor airborne transmission and improving indoor air quality. Environ. Res. 213, 113579 https://doi.org/10.1016/j.envres.2022.113579.

Nicas, M., Nazaroff, W.W., Hubbard, A., 2005. Toward understanding the risk of secondary airborne infection: emission of respirable pathogens. J. Occup. Environ. Hyg. 2 (3), 143–154. https://doi.org/10.1080/15459620590918466.

Nielsen, P.V., 1993. Displacement Ventilation. PhD Thesis,. Aalborg University, Denmark.

Noakes, C.J., Beggs, C.B., Sleigh, P.A., 2004. Modelling the performance of upper-room ultraviolet germicidal irradiation devices in ventilated rooms: comparison of analytical and CFD methods. Indoor Built Environ. 13 (6), 477–488. https://doi.org/10.1177/1420326X04049343.

Noakes, C.J., Sleigh, P.A., Fletcher, L.A., Beggs, C.B., 2006. Use of CFD modelling to optimise the design of upper-room UVGI disinfection systems for ventilated rooms. Indoor Built Environ. 15 (4), 347–356.

Norbäck, D., Wieslander, G., Zhang, X., Zhao, Z., 2011. Respiratory symptoms, perceived air quality and physiological signs in elementary school pupils in relation to displacement and mixing ventilation system: an intervention study. Indoor Air 21 (5), 427–437. https://doi.org/10.1111/j.1600-0668.2011.00717.x.

Novoselac, A., Srebric, J., 2003. Comparison of air exchange efficiency and contaminant removal effectiveness as IAQ indices. Trans. Am. Soc. Heat. Refrig. Air Cond. Eng. 109 (2), 339–349.

Park, S., Choi, Y., Song, D., Kim, E.K., 2021. Natural ventilation strategy and related issues to prevent coronavirus disease 2019 (COVID-19) airborne transmission in a school building. Sci. Total Environ. 789, 147764 https://doi.org/10.1016/j.scitotenv.2021.147764.

Park, S., Mistrick, R., Rim, D., 2022. Performance of upper-room ultraviolet germicidal irradiation (UVGI) system in learning environments: effects of ventilation rate, UV fluence rate, and UV radiating volume. Sustain. Cities Soc. 104048 https://doi.org/10.1016/j.scs.2022.104048.

Pei, G., Rim, D., 2021. Quality control of computational fluid dynamics (CFD) model of ozone reaction with human surface: effects of mesh size and turbulence model. Build. Environ. 189, 107513 https://doi.org/10.1016/j.buildenv.2020.107513.

Pei, G., Taylor, M., Rim, D., 2021. Human exposure to respiratory aerosols in a ventilated room: effects of ventilation condition, emission mode, and social distancing. Sustain. Cities Soc. 103090 https://doi.org/10.1016/j.scs.2021.103090.

Pichurov, G., Srebric, J., Zhu, S., Vincent, R.L., Brickner, P.W., Rudnick, S.N., 2015. A validated numerical investigation of the ceiling fan's role in the upper-room UVGI efficacy. Build. Environ. 86, 109–119. https://doi.org/10.1016/j.buildenv.2014.12.021.

Prather, K.A., Wang, C.C., Schooley, R.T., 2020. Reducing transmission of SARS-CoV-2. Science 368 (6498), 1422–1424. https://doi.org/10.1126/science.abc6197.

Raeiszadeh, M., Adeli, B., 2020. A critical review on ultraviolet disinfection systems against COVID-19 outbreak: applicability, validation, and safety considerations. ACS Photon. 7 (11), 2941–2951. https://doi.org/10.1021/acsphotonics.0c01245.

Ren, C., Zhu, H.C., Cao, S.J., 2022. Ventilation strategies for mitigation of infection disease transmission in an indoor environment: a case study in office. Buildings 12 (2), 180. https://doi.org/10.3390/buildings12020180.

Rim, D., Novoselac, A., 2009. Transport of particulate and gaseous pollutants in the vicinity of a human body. Build. Environ. 44 (9), 1840–1849. https://doi.org/10.1016/j.buildenv.2008.12.009.

Rim, D., Novoselac, A., 2010. Ventilation effectiveness as an indicator of occupant exposure to particles from indoor sources. Build. Environ. 45 (5), 1214–1224. https://doi.org/10.1016/j.buildenv.2009.11.004.

Rim, D., Novoselec, A., Morrison, G., 2009. The influence of chemical interactions at the human surface on breathing zone levels of reactants and products. Indoor Air 19 (4), 324. https://doi.org/10.1111/j.1600-0668.2009.00595.x.

Rudnick, S.N., McDevitt, J.J., Hunt, G.M., Stawnychy, M.T., Vincent, R.L., Brickner, P. W., 2015. Influence of ceiling fan's speed and direction on efficacy of upper-room, ultraviolet germicidal irradiation: experimental. Build. Environ. 92, 756–763. https://doi.org/10.1016/j.buildenv.2014.03.025.

Shan, W., Rim, D., 2018. Thermal and ventilation performance of combined passive chilled beam and displacement ventilation systems. Energy Build. 158, 466–475. https://doi.org/10.1016/j.enbuild.2017.10.010.

Sheikhnejad, Y., Aghamolaei, R., Fallahpour, M., Motamedi, H., Moshfeghi, M., Mirzaei, P.A., Bordbar, H., 2022. Airborne and aerosol pathogen transmission modeling of respiratory events in buildings: an overview of computational fluid dynamics. Sustain. Cities Soc. 103704 https://doi.org/10.1016/j.scs.2022.103704.

Sosnowski, M., Krzywanski, J., Grabowska, K., Gnatowska, R., 2018. Polyhedral meshing in numerical analysis of conjugate heat transfer. EPJ Web Conf. 180, 02096. https://doi.org/10.1051/epjconf/201818002096.

Srivastava, S., Zhao, X., Manay, A., Chen, Q., 2021. Effective ventilation and air disinfection system for reducing coronavirus disease 2019 (COVID-19) infection risk in office buildings. Sustain. Cities Soc. 75, 103408 https://doi.org/10.1016/j.scs.2021.103408.

Su, W., Yang, B., Melikov, A., Liang, C., Lu, Y., Wang, F., Kosonen, R., 2022. Infection probability under different air distribution patterns. Build. Environ. 207, 108555 https://doi.org/10.1016/j.buildenv.2021.108555.

Tang, J.W., Marr, L.C., Li, Y., Dancer, S.J., 2021. Covid-19 has redefined airborne transmission. bmj 373. https://doi.org/10.1136/bmj.n913.

Tian, L., Lin, Z., Wang, Q., 2010. Comparison of gaseous contaminant diffusion under stratum ventilation and under displacement ventilation. Build. Environ. 45 (9), 2035–2046. https://doi.org/10.1016/j.buildenv.2010.01.002.

Walker, C.M., Ko, G., 2007. Effect of ultraviolet germicidal irradiation on viral aerosols. Environ. Sci. Technol. 41 (15), 5460–5465. https://doi.org/10.1021/es070056u.

Wang, Y., Zhao, F.Y., Kuckelkorn, J., Liu, D., Liu, J., Zhang, J.L., 2014. Classroom energy efficiency and air environment with displacement natural ventilation in a passive public school building. Energy Build. 70, 258–270. https://doi.org/10.1016/j.enbuild.2013.11.071.

Whalen, J., 2009. Environmental Control for Tuberculosis: Basic Upper Room Ultraviolet Germicidal Irradiation Guidelines for Health Care Settings. National Institutes of Occupational Safety and Health, Cincinnati, OH. Report No. DHHS (NIOSH), publication No. 2009-015. https://stacks.cdc.gov/view/cdc/5306.

Wilson, N., Corbett, S., Tovey, E., 2020. Airborne transmission of covid-19. bmj 370. https://doi.org/10.1136/bmj.m3206.

Xu, C., Liu, W., Luo, X., Huang, X., Nielsen, P.V., 2022. Prediction and control of aerosol transmission of SARS-CoV-2 in ventilated context: from source to receptor. Sustain. Cities Soc. 76, 103416 https://doi.org/10.1016/j.scs.2021.103416.

Zhang, H., Li, D., Xie, L., Xiao, Y., 2015. Documentary research of human respiratory droplet characteristics. Procedia Eng. 121, 1365–1374. https://doi.org/10.1016/j.proeng.2015.09.023.

Zhou, M., Zou, J., 2021. A dynamical overview of droplets in the transmission of respiratory infectious diseases. Phys. Fluids 33 (3), 031301. https://doi.org/10.1063/5.0039487.

Zhu, S., Srebric, J., Rudnick, S.N., Vincent, R.L., Nardell, E.A., 2013. Numerical investigation of upper-room UVGI disinfection efficacy in an environmental chamber with a ceiling fan. Photochem. Photobiol. 89 (4), 782–791. https://doi.org/10.1111/php.12039.

Zhu, S., Lin, T., Wang, L., Nardell, E.A., Vincent, R.L., Srebric, J., 2022. Ceiling impact on air disinfection performance of Upper-Room Germicidal Ultraviolet (UR-GUV). Build. Environ. 224, 109530 https://doi.org/10.1016/j.buildenv.2022.109530.